

Technical Report: A Hybrid Systems Model of Feedback Optimization for Linear Systems

Oscar Jed R. Chuy¹, Matthew T. Hale¹, and Ricardo G. Sanfelice²

Abstract—Feedback optimization algorithms compute inputs to a system in real time, which helps mitigate the effects of unknown disturbances. However, existing work models both system dynamics and computations in either discrete or continuous time, which does not faithfully model some applications. In this work, we model linear system dynamics in continuous time, and we model the computations of inputs in discrete time. Therefore, we present a novel hybrid systems framework for modeling feedback optimization of linear time-invariant systems that are subject to unknown, constant disturbances. For this setup, we first establish the well-posedness of the hybrid model and establish completeness of solutions while ruling out Zeno behavior. Then, our main result derives a convergence rate and an error bound for the full hybrid computation-in-the-loop system and shows that it converges exponentially towards a ball of known radius about a desired fixed point. Simulation results show that this approach successfully mitigates the effects of disturbances, with the magnitude of steady-state error being 81% less than the magnitude of the disturbances in the system.

I. INTRODUCTION

Many automation tasks require optimizing the behavior of a dynamical system, which often involves solving a planning problem offline. When solving such problems with accurate system models, an optimization problem may be solved in a feedforward configuration to generate optimal waypoints or trajectories that are used to drive the system in question. This approach has been applied in chemical processes, power systems, energy networks, voltage regulation, and congestion control in communication systems, among others [1]–[3]. However, errors or approximations in the model can lead to sub-optimal solutions [1] because the inputs applied to a system do not actually produce the outputs that one intends.

If models are inaccurate, one alternative approach called “feedback optimization” instead *measures* system outputs [4], and then optimizes inputs based on those measurements, rather than based on predictions of outputs that come from a possibly inaccurate model. This setup embeds an optimization algorithm in a feedback loop, and it (i)

measures system outputs in real time, (ii) feeds those outputs into a running optimization algorithm, (iii) performs some computations to drive the values of inputs toward their optimal values, and (iv) applies those inputs to the system. In such systems, instead of attempting to optimize *a priori* with an inaccurate dynamical model and then regulate to the resulting trajectory, the optimization and regulation are both done online, which makes it possible for the system and optimization algorithm to react to disturbances.

Feedback optimization has been shown to have several benefits: it is robust to inaccurate system models and time-varying parameters, achieves constraint satisfaction with minimal model dependence, and eliminates the need for pre-computed set points or reference signals [1]. This approach has been used, for example, in decentralized settings [3], [5], gradient-based feedback control [6], momentum-based controllers [6], primal-dual saddle-point flow optimization [6], projected saddle-flows as feedback controllers [1], zeroth-order optimization [1], and Bayesian-based optimization [1].

In existing work, feedback optimization has been applied to systems with either (a) continuous-time dynamics and a continuous-time optimization algorithm in the loop or (b) discrete-time dynamics and a discrete-time optimization algorithm in the loop [1], [7]–[9]. However, physical systems are often naturally modeled in continuous time and digital computers are naturally modeled in discrete time, which means that the practical implementation of such algorithms can produce dynamics that are not captured by (a) or (b).

Therefore, in this paper we seek to show that feedback optimization can be performed in practical settings with continuous-time dynamics using discrete-time optimization, while retaining key benefits like disturbance rejection. To faithfully model such a setup, we are naturally led to a hybrid systems model of feedback optimization. We emphasize that we are not the first to use feedback optimization. Instead, we are, to the best of our knowledge, the first to present a hybrid systems model of feedback optimization, which we argue is the natural setting for practical implementations that consider physical systems driven by digital computers.

The contributions of this paper are the following:

- We model feedback optimization as a hybrid system and show that (i) it is free from Zeno behavior and (ii) all maximal solutions are complete, i.e., there are no theoretical obstructions to the system running for arbitrarily long periods of time (Proposition 1).
- We bound the finite-time distance between the state of the hybrid feedback optimization model and a desired goal state (Theorem 1).

¹School of Electrical and Computer Engineering, Georgia Institute of Technology, Atlanta, GA USA. Emails: {ochuy3, matthale}@gatech.edu.

²School of Electrical and Computer Engineering, University of California, Santa Cruz, CA USA. Email: ricardo@ucsc.edu.

All authors were supported by AFOSR under grant FA9550-19-1-0169. Chuy and Hale were supported by ONR under grants N00014-21-1-2495 and N00014-22-1-2435, and AFRL under grants FA8651-22-F-1052 and FA8651-23-F-A006. Sanfelice was supported by NSF Grants no. CNS-2039054 and CNS-2111688, by AFOSR Grants nos. FA9550-23-1-0145, FA9550-23-1-0313, and FA9550-23-1-0678, by AFRL Grant nos. FA8651-22-1-0017 and FA8651-23-1-0004, by ARO Grant no. W911NF-20-1-0253, and by DoD Grant no. W911NF-23-1-0158.

- We bound the steady-state distance between the state of the hybrid feedback optimization model and a desired goal state (Corollary 1).
- We show in simulation that hybrid feedback optimization successfully rejects disturbances by producing a steady-state error whose magnitude is 81% less than that of unknown system disturbances (Section VI).

The rest of the paper is organized as follows. Section II provides notation and background. Section III models feedback optimization as a hybrid system, and Section IV derives properties of its solutions. Then Section V establishes the solutions' approximate convergence to a fixed point. Simulations are presented in Section VI, and Section VII concludes.

II. PRELIMINARIES AND PROBLEM FORMULATION

A. Notation

Let \mathbb{R} be the set of real numbers and let \mathbb{N} be the set of non-negative integers. For a differentiable objective function $\Phi : \mathbb{R}^m \times \mathbb{R}^p \rightarrow \mathbb{R}$, let $\nabla_u \Phi$ and $\nabla_y \Phi$ represent the partial derivatives with respect to its first and second arguments, respectively. The symbol I_n denotes the identity matrix of dimension n . The 2-norm of a vector x is denoted $\|x\|$. For a non-empty, compact, convex set \mathcal{Z} , the symbol $\Pi_{\mathcal{Z}}[v]$ denotes the Euclidean projection of a point v onto \mathcal{Z} , i.e., $\Pi_{\mathcal{Z}}[v] = \arg \min_{z \in \mathcal{Z}} \|v - z\|$. We use $\lambda_i(N)$ to denote the i^{th} eigenvalue of a matrix N , and we use $\Re\{z\}$ to denote the real part of a complex number z . We also write $\lambda_{\min}(N)$ for the smallest (real) eigenvalue of a symmetric matrix N . Given $r \geq 0$, we use $B_r(0) := \{x \in \mathbb{R}^n : \|x\| \leq r\}$ to denote the closed Euclidean ball of radius r about the origin in \mathbb{R}^n . For a set S and a point x , we use $\|x\|_S := \inf_{s \in S} \|x - s\|$. We also write $d_{\mathcal{U}} = \max_{u_1, u_2 \in \mathcal{U}} \|u_1 - u_2\|$ as the diameter of the set \mathcal{U} .

B. Feedback Optimization Background and Setup

In this section we review the conventional formulation of feedback optimization; for surveys on this subject, see [1], [10]. At a high level, feedback optimization uses real-time measurements from a dynamical system that are fed into an optimization algorithm in a closed-loop structure. One goal in doing so is to optimize the steady-state behavior of the dynamical system. This setup provides robustness to inaccurate problem data such as system model errors, and it also provides robustness to time-varying parameters [1]. Additionally, this setup ensures that a system reacts to disturbances, which helps to reject additive disturbances and uncertainties.

To elaborate, suppose that we have a linear time invariant (LTI) system with dynamics

$$\begin{aligned} \dot{x} &= Ax + Bu \\ y &= \Psi x + d, \end{aligned} \quad (1)$$

where $x \in \mathbb{R}^n$ is the system's state, $u \in \mathcal{U} \subset \mathbb{R}^m$ is its input that is constrained to lie in the non-empty, compact, convex set \mathcal{U} , and $y \in \mathbb{R}^p$ is its output. The vector $d \in \mathbb{R}^p$ is a constant, unknown, and unmodeled disturbance (e.g., bias)

in the system, which is a typical component of feedback optimization problem formulations [1]–[3], [6], [7]. Such disturbances arise for example in AC optimal power flow optimization [1], [2], [6] and voltage control for DC power systems [3], [7]. Regarding the system itself, we impose the following assumption.

Assumption 1. The matrix A in (1) is Hurwitz.

Assumption 1 implies that the matrix A from (1) is invertible, which is standard in the setting of feedback optimization [1], [11], [12]. The steady-state input-to-output map for the system in (1) is defined as

$$y := Hu + d, \quad (2)$$

where $H := -\Psi A^{-1}B$ is the sensitivity matrix of the system in (1).

To optimize the steady-state behavior of this system with constraints on u , one can drive the system's input and output to a solution of the optimization problem

$$\min_{u, y} \Phi(u, y) \quad (3a)$$

$$\begin{aligned} \text{subject to } & y = Hu + d \\ & u \in \mathcal{U}, \quad y \in \mathbb{R}^p, \end{aligned} \quad (3b)$$

where \mathcal{U} is a non-empty, compact, convex set defining the constraints for u and $\Phi : \mathbb{R}^m \times \mathbb{R}^p \rightarrow \mathbb{R}$ is an objective function. By incorporating the constraint (3b) into (3a), one could reduce this problem to

$$\begin{aligned} \min_u \quad & \tilde{\Phi}(u) \\ \text{subject to } & u \in \mathcal{U}, \end{aligned}$$

where $\tilde{\Phi}(u) := \Phi(u, Hu + d)$.

However, this problem cannot be solved in this form in practice because the substitution $y = Hu + d$ would require exact knowledge of the constant disturbance d , which is not available in general. Instead, feedback optimization is employed to (i) measure the output y , which will be subject to the disturbance d , (ii) then optimize over u , and (iii) apply the resulting u as the input to the system. This process recurs over time, i.e., an output is measured, an input is computed and applied to the system, then a subsequent output is measured and a new input is computed and applied to the system, etc. In this work, measurements of y are taken and used in the computations of u , and therefore y is sampled at certain discrete instants of time. We use the symbol y_s to denote the sampled value of y that is used when optimizing over u .

Remark 1. Although the underlying dynamical system need not always be at steady-state, we will approximate the value of a sampled output y_s as coming from the steady-state map $y_s = Hu + d$ when the input to the system is u . This approximation is justified, for example, when the LTI dynamics of the system converge sufficiently quickly. The use of this approximation is common in the feedback optimization literature [3], [6], [11], and we therefore incorporate it into the hybrid model that we formulate.

As in the existing feedback optimization literature, we use this formulation to define a closed-loop system that connects the LTI system with a controller that uses a gradient-based optimization algorithm. This algorithm computes successive inputs that are the iterates of an optimization algorithm that minimizes $\tilde{\Phi}$. We impose the following assumption about the objective function that is optimized.

Assumption 2. The objective Φ takes the form

$$\Phi(u, y) = \frac{1}{2}u^\top Q_u u + \frac{1}{2}y^\top Q_y y,$$

where $Q_u \in \mathbb{R}^{m \times m}$ and $Q_y \in \mathbb{R}^{p \times p}$ are symmetric and positive definite.

This type of quadratic objective is widely used in the feedback optimization literature [1], [12], and it implies that the gradient of Φ with respect to u at the point (u, y_s) is equal to

$$\nabla_u \Phi(u, y_s) = Q_u u + H^\top Q_y y_s, \quad (5)$$

where we have used the approximation $y_s = Hu + d$ from Remark 1. Using that same remark, the Hessian of Φ with respect to u at the point (u, y_s) is equal to

$$\nabla_u^2 \Phi(u, y_s) = Q_u + H^\top Q_y H,$$

which satisfies

$$\lambda_{\min}(Q_u + H^\top Q_y H) \geq \lambda_{\min}(Q_u) > 0, \quad (6)$$

which follows from Weyl's inequalities, e.g., [13, Corollary 4.3.12], and the fact that Q_u is symmetric and positive definite under Assumption 2.

Therefore, under the approximation $y_s = Hu + d$ from Remark 1, the function $\tilde{\Phi}$ is $\lambda_{\min}(Q_u)$ -strongly convex and $\nabla_u \tilde{\Phi}$ is L -Lipschitz for

$$L = \lambda_{\max}(Q_u) + \lambda_{\max}(H^\top Q_y H). \quad (7)$$

Going forward, to explicitly account for the timing with which new values of u are computed and new values of y_s are sampled, we will continue to write $\Phi(u, y_s)$ in place of $\tilde{\Phi}(u)$. We emphasize that these two functions are the same under Remark 1, and, in particular, the function Φ is $\lambda_{\min}(Q_u)$ -strongly convex in u and has an L -Lipschitz gradient with respect to u for the same L in (7).

Using the above gradient, when samples y_s are provided, a gradient-based feedback controller can be written as

$$u_{k+1} = \Pi_{\mathcal{U}}[u_k - \gamma \nabla_u \Phi(u_k, y_s)], \quad (8)$$

where u_k is the k^{th} iteration of the algorithm solving the optimization problem.

Then, at a high level, the closed-loop interconnected LTI system is given as

$$\begin{aligned} \text{Plant: } \begin{cases} \dot{x} &= Ax + Bu \\ y &= \Psi x + d, \end{cases} \\ \text{Controller: } u_{k+1} &= \Pi_{\mathcal{U}}[u_k - \gamma \nabla_u \Phi(u_k, y_s)], \end{aligned} \quad (9)$$

which evolves as follows. First, a constant input u_0 is applied to the system. Second, the output of the system is measured, giving y_s . Third, the optimization algorithm (8) is used to compute a sequence of iterates that works toward the solution of the problem in (3), though it may not reach an optimum. Fourth, after some period of time (to be defined later), the most recent iterate of the optimization algorithm is used as the next constant input to the system, i.e., we set $u = u_k$, and then this process repeats, which gives the system a piecewise constant input over time.

While Assumption 1 alone is insufficient to guarantee closed-loop stability, other works have shown that stability can be guaranteed under the use of sufficiently small step sizes in the optimization-based controller [1], [7]. Such works consider discrete-time systems with discrete-time optimization algorithms, and the use of small step sizes provides a form of timescale separation. In this work, we will show that an analogous form of timescale separation provides similar benefits through the proposed hybrid model approach.

As mentioned in the introduction, it is standard in the feedback optimization literature for the system dynamics and the optimization-based controller to both be modeled in either discrete time or continuous time. To the best of our knowledge there has not been a systematic investigation of hybrid feedback optimization for a continuous-time system driven by discrete-time computations. Other existing work has developed hybrid models of optimization algorithms [14]–[16], though the current paper differs by developing a hybrid model of a continuous-time system with a discrete-time optimization algorithm in the loop. There has also been work on hybrid model predictive control that incorporates continuous and discrete dynamics [17], but our aim is different because we implement a hybrid framework for feedback optimization. The next section provides background on hybrid systems.

C. Background on Hybrid Systems

A hybrid system is one that exhibits both continuous-time and discrete-time behaviors. In this paper, a hybrid system \mathcal{H} takes the form

$$\mathcal{H} = \begin{cases} \dot{\zeta} \in F(\zeta) & \zeta \in C \\ \zeta^+ \in G(\zeta) & \zeta \in D \end{cases},$$

where $\zeta \in \mathbb{R}^n$ is the system's state vector and the maps F and G are set-valued in general. The function F defines the flow map and governs the continuous dynamics within the flow set C , while G defines the jump map, which models the system's discrete behavior within the jump set D .

Definition 1 (Hybrid Basic Conditions [18]). A hybrid system \mathcal{H} with data (C, F, D, G) satisfies the hybrid basic conditions if

- 1) C and D are closed subsets of \mathbb{R}^n ;
- 2) $F : \mathbb{R}^n \rightrightarrows \mathbb{R}^n$ is outer semicontinuous¹, and locally

¹A set-valued mapping $M : \mathbb{R}^m \rightrightarrows \mathbb{R}^n$ is outer semicontinuous (osc) at $x \in \mathbb{R}^m$ if for every sequence of points $\{x_i\}_{i \in \mathbb{N}}$ convergent to x and any convergent sequence of points $\{y_i\}_{i \in \mathbb{N}}$ with $y_i \in M(x_i)$, one has $y \in M(x)$, where $\lim_{i \rightarrow \infty} y_i = y$ [18].

bounded² relative to C , $C \subset \text{dom } F$, and $F(\zeta)$ is convex for every $\zeta \in C$

- 3) $G : \mathbb{R}^n \rightrightarrows \mathbb{R}^n$ is outer semicontinuous and locally bounded relative to D , and $D \subset \text{dom } G$.

If a hybrid system satisfies the hybrid basic conditions, then it is well-posed by [18, Theorem 6.30], meaning that errors in the models of F and G up to a certain threshold produce bounded changes in the resulting system trajectories. It is not automatic to formulate a well-posed hybrid system, and this paper will do so for a hybrid model of feedback optimization, in addition to analyzing its properties and performance.

For a hybrid system \mathcal{H} , its solutions, denoted by ϕ , are hybrid arcs that can in general be maximal³, complete⁴, and Zeno⁵.

D. Problem Formulation

The rest of the paper will solve the following problems.

Problem 1. Formulate a hybrid feedback optimization model of the plant and controller in (9) that explicitly accounts for (i) how system outputs are intermittently measured and used in the optimization-based controller and (ii) how inputs are computed and applied to the system. Show that the hybrid model is well-posed.

Problem 2. Prove the convergence of the system toward an equilibrium, and bound the steady-state error in terms of the disturbance d .

III. A HYBRID MODEL FOR FEEDBACK OPTIMIZATION

This section formulates the hybrid system model of feedback optimization, which partially solves Problem 1. We first give an overview of the necessary features of the hybrid model that we formulate, then we specify its mathematical form.

A. Overview of Hybrid Feedback Optimization

The continuous-time system in (1) receives inputs from the discrete-time optimization algorithm in (8), and those inputs only change when the optimization algorithm generates new inputs for the system to use. Between these changes, inputs applied to the system are held constant. In other words, the inputs to the system in (1) are piecewise constant. Similarly, the optimization algorithm measures an output of the system and uses it to perform some number of computations to optimize inputs. This sampled value of the output is held constant by the optimization algorithm while optimizing an input, and that output value does not change until a new output is sampled, at which point the value of the old output is overwritten and computations towards a new input begin.

²A set-valued mapping $M : \mathbb{R}^m \rightrightarrows \mathbb{R}^n$ is locally bounded at $x \in \mathbb{R}^m$ if there is a neighborhood U_x of x such that $M(U_x) \subset \mathbb{R}^n$ is bounded [18].

³A solution ϕ to \mathcal{H} is maximal if there does not exist another solution ψ to \mathcal{H} such that $\text{dom } \phi$ is a proper subset of $\text{dom } \psi$ and $\phi(t, j) = \psi(t, j)$ for all $(t, j) \in \text{dom } \phi$ [18].

⁴The solution ϕ is complete if $\text{dom } \phi$ is unbounded, i.e., if $\text{length}(\text{dom } \phi) = \sup_t \text{dom } \phi + \sup_j \text{dom } \phi = \infty$ [18].

⁵The solution ϕ is Zeno if it is complete and $\sup_t \text{dom } \phi < \infty$ [18].

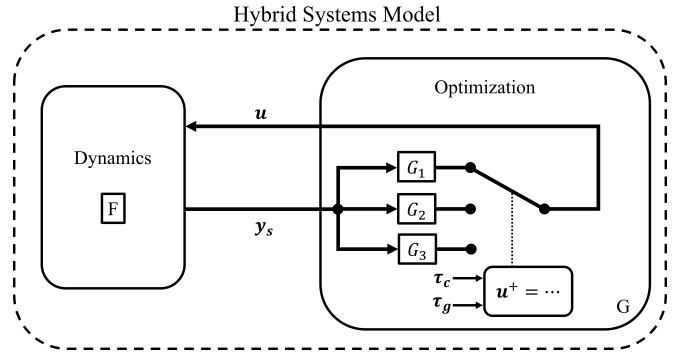


Fig. 1. A visual representation of the hybrid framework for feedback optimization. The LTI system dynamics are encoded in the flow map F , while computations in the loop, the act of sampling the output, and the act of changing the input to the LTI system are all modeled using the jump map G . The sampled output y_s is the only piece of information that passes from the system to the optimization algorithm in the loop, and the input u is the only piece of information that passes from the optimization algorithm to the system.

We mathematically model these properties as follows. The flow map F from Definition 1 will model the LTI system dynamics in (1) with piecewise constant inputs. The jump map G from Definition 1 will model both the sampling of outputs and the application of new inputs to the system. It will also model the computation of intermediate iterates by the optimization algorithm, which are generated at discrete points in time between the points in time at which the output value is sampled. This setup is visually represented in Figure 1.

B. Hybrid Modeling and Flow and Jump Sets

To solve Problem 1, a hybrid model must account for the behaviors of the continuous-time LTI system and the underlying discrete-time optimization algorithm. To account for the behaviors of the LTI system, we will define the state of the hybrid system to include both the state and the input of the LTI system dynamics in (1). In addition, we will define other states of the hybrid system that include the values of outputs sampled from the system and the intermediate iterates of the computations of the optimization algorithm in the loop. To jointly model these behaviors, we must also track how much continuous time elapses between successive computations by the optimization algorithm, as well as the amount of time that elapses when each input is applied to the system.

Accounting for all of these factors, the state of the hybrid system is

$$\zeta := \begin{pmatrix} x^\top & u^\top & y_s^\top & z^\top & \tau_c & \tau_g & \ell \end{pmatrix}^\top,$$

where $x \in \mathbb{R}^n$ and $u \in \mathbb{R}^m$ are, respectively, the state and input of the LTI system in (1). The vector $y_s \in \mathbb{R}^p$ is the value of the sampled output of the LTI system that is used in the underlying optimization algorithm, $z \in \mathbb{R}^m$ is the current iterate of that optimization algorithm, $\tau_c \in \mathbb{R}$ is a timer that tracks the amount of continuous time left until the input to the system changes, $\tau_g \in \mathbb{R}$ is a timer that accounts for the

amount of continuous time needed to complete each iteration of the optimization algorithm, and $\ell \in \mathbb{N}$ is a counter that tracks the number of iterations of the optimization algorithm that are completed between successive changes in the input to the system. Thus, the full state is $\zeta \in \mathbb{R}^n \times \mathbb{R}^m \times \mathbb{R}^p \times \mathbb{R}^m \times \mathbb{R} \times \mathbb{R} \times \mathbb{N}$, and we will treat it as $\zeta \in \mathcal{X} := \mathbb{R}^{n+2m+p+3}$.

The timers τ_c and τ_g count down from some positive number to zero, and jumps occur only when they reach zero. Then, the state is allowed to flow while both $\tau_c > 0$ and $\tau_g > 0$, and the state is in the jump set when $\tau_c = 0$ or $\tau_g = 0$. Formally, these conditions are captured by the flow set C and jump set D defined as

$$\begin{aligned} C &:= \{\zeta \in \mathcal{X} \mid \tau_c \in [0, \tau_{c,\max}], \tau_g \in [0, \tau_{g,\text{comp}}]\} \\ D &:= \{\zeta \in \mathcal{X} \mid \tau_c = 0 \text{ or } \tau_g = 0\}. \end{aligned} \quad (10)$$

C. Flow Map Definition

The flow map is derived from (1), which describes how the state x continuously evolves over time. We note that y_s , the sampled output used by the optimization algorithm, does not vary continuously, as it is measured at certain time instants and is held constant between measurements. The timers τ_c and τ_g count down to zero continuously and with unit rate, while all other states only change during jumps. Therefore, the flow map is

$$\dot{\zeta} = F(\zeta) := \begin{pmatrix} Ax + Bu \\ 0 \\ 0 \\ 0 \\ -1 \\ -1 \\ 0 \end{pmatrix}. \quad (11)$$

D. Jump Map Definition

The jump map has three distinct cases based on the conditions in the jump set: (i) $\tau_g = 0$ with $\tau_c > 0$, (ii) $\tau_c = 0$ with $\tau_g > 0$, and (iii) $\tau_c = \tau_g = 0$. Recall from above that τ_g models the amount of continuous time that is required to complete a single iteration of the underlying gradient descent algorithm, while τ_c models the amount of time left until a new input is applied to the system.

We begin with Case (i). We use the constant $\tau_{g,\text{comp}}$ to denote the amount of continuous time that is required to complete a single gradient descent iteration, and τ_g counts down from this value to zero. Thus, we have $\tau_g \in [0, \tau_{g,\text{comp}}]$. In Case (i), where only $\tau_g = 0$, a single gradient descent step has been completed when the jump occurs, but since $\tau_c > 0$, the timer for changing the system input is still counting down, and the current iterate z is not yet applied as the system input. Thus, the jump map for this case updates the state z using a gradient step, i.e.,

$$\begin{aligned} z^+ &= \Pi_{\mathcal{U}}[z - \gamma \nabla_u \Phi(z, y_s)] \\ &= \Pi_{\mathcal{U}}[z - \gamma (\nabla \Phi_u(z) + H^\top \nabla \Phi_y(y_s))], \end{aligned}$$

where $\gamma > 0$ is a stepsize and we have used (5) to expand the gradient. Here $y_s \in \mathbb{R}^p$ is the most recent sample of the system output that the optimization algorithm has taken.

Additionally, the jump map for this case resets τ_g to $\tau_{g,\text{comp}}$, and the counter of completed iterations is incremented by 1, i.e., the jump map sets $\ell^+ = \ell + 1$. The jump map for this case is denoted G_1 and is defined as

$$G_1(\zeta) = \begin{pmatrix} x \\ u \\ y_s \\ \Pi_{\mathcal{U}}[z - \gamma \mu] \\ \tau_c \\ \tau_{g,\text{comp}} \\ \ell + 1 \end{pmatrix}, \quad (12)$$

where

$$\mu = \nabla \Phi_u(z) + H^\top \nabla \Phi_y(y_s).$$

In case (ii), when $\tau_c = 0$ and $\tau_g > 0$, a new input is applied to the system, a new output is sampled, and the timer τ_c resets. Specifically, the timer τ_c resets to some point in the interval $[\tau_{c,\min}, \tau_{c,\max}]$, where $0 < \tau_{c,\min} < \tau_{c,\max}$, where this range of times represents indeterminacy in the amount of time that elapses between the application of successive inputs to the system. We require that $2\tau_{g,\text{comp}} < \tau_{c,\min}$, which ensures that, when the system is properly initialized, at least two gradient descent iterations are performed between any consecutive changes in the value of the input. When the input changes, it is set equal to the current optimization iterate, which is stored in z . When τ_c reaches 0, the value of y at that point in time is sampled and stored in the state y_s , which is held constant until the next sample. This measurement is subject to the disturbance d from (2), which is unknown. The counter ℓ is reset to 0; since a new output has just been sampled, the computation of a new input is about to begin, and zero iterations have been completed, which gives $\ell = 0$. The jump map for this case is denoted G_2 and is defined as

$$G_2(\zeta) = \begin{pmatrix} x \\ z \\ Hu + d \\ z \\ [\tau_{c,\min}, \tau_{c,\max}] \\ \tau_g \\ 0 \end{pmatrix}, \quad (13)$$

where, as described in Remark 1, we approximate the output $y_s = Cx + d$ with the steady state mapping $y_s = Hu + d$; the unknown, constant disturbance d is treated as a parameter and not a state, and thus it appears in the map G_2 but is not an element of the state vector ζ . In the map G_2 , the state z jumps to z . This jump encodes the fact that if the input to the LTI system changes while a gradient descent iteration is being computed, then the gradient descent iteration that was in progress is stopped, and, instead, when the input to the system is changed, a new gradient descent iteration begins from the point at which the previous one had begun, but with the new value of y_s used in its computations.

In case (iii), where both $\tau_c = 0$ and $\tau_g = 0$, we combine cases (i) and (ii). To model this case, the system first jumps using one of the jump maps and then jumps using the other.

That is, it executes G_1 and then G_2 , or it executes G_2 and then G_1 .

Formally, the full jump map G is defined as

$$\zeta^+ \in G(\zeta) := \begin{cases} G_1(\zeta) & \text{if } \tau_c > 0 \text{ and } \tau_g = 0 & \text{Case (i)} \\ G_2(\zeta) & \text{if } \tau_c = 0 \text{ and } \tau_g > 0 & \text{Case (ii)} \\ G_3(\zeta) & \text{if } \tau_c = 0 \text{ and } \tau_g = 0 & \text{Case (iii)}, \end{cases} \quad (14)$$

where

$$G_3(\zeta) = G_1(\zeta) \cup G_2(\zeta),$$

and where G_1 is from (12) and G_2 is from (13).

The jump set D can be rewritten as

$$D = D_1 \cup D_2, \quad (15)$$

where

$$D_1 = \{\zeta \in \mathcal{X} : \tau_g = 0\} \quad (16)$$

$$D_2 = \{\zeta \in \mathcal{X} : \tau_c = 0\}. \quad (17)$$

Now we can fully define the hybrid model of feedback optimization as

$$\mathcal{H}_{FO} := (C, F, D, G), \quad (18)$$

where C is from (10), F is from (11), D is from (15), and G is from (14). While \mathcal{H}_{FO} has been defined, we still must show that it is well-posed and that its solutions are well-defined. This analysis is done in the next section.

IV. PROPERTIES OF HYBRID FEEDBACK OPTIMIZATION

In this section, we show that the hybrid feedback optimization system \mathcal{H}_{FO} satisfies certain technical conditions that ensure that its solutions exist for all time, which completes our solution to Problem 1. Then we describe how to initialize \mathcal{H}_{FO} and model the evolution of solutions to \mathcal{H}_{FO} over time.

A. Well-Posedness and Existence of Solutions

Toward establishing that solutions to \mathcal{H}_{FO} are defined for all time, we have the following.

Lemma 1. The hybrid feedback optimization model \mathcal{H}_{FO} in (18) is well-posed in the sense of Definition 1.

Proof. By inspection, the set C in (10) and the set D in (15) together satisfy Condition 1 in Definition 1. The map F in (11) is defined everywhere on C and outputs a singleton that is a linear function of the state, and thus it satisfies Condition 2 in Definition 1.

To show that the map G in (14) satisfies Condition 3, we can use Lemma 4 in Appendix A. The jump map G_1 in (12) is outer semicontinuous because the projection mapping $\Pi_{\mathcal{U}}[\cdot]$ is C^0 and because G_1 outputs a singleton. The jump map G_2 in (13) is outer semicontinuous because its only set-valued entry outputs a compact interval and all other entries output singletons. Then the feedback optimization jump map in (14) has the structure of the jump map in Lemma 4, and the feedback optimization jump set in (15) has

the same structure as the jump set in Lemma 4. Therefore, using Lemma 4, we see that the feedback optimization jump map G in (14) is both outer semicontinuous and locally bounded relative to the closed set D . Then Condition 3 of Definition 1 is satisfied. Therefore, all conditions of Definition 1 are satisfied, and the system \mathcal{H}_{FO} is well-posed. \square

The following result shows that all maximal solutions to the system \mathcal{H}_{FO} are complete.

Proposition 1 (Completeness of Maximal Solutions). Consider the hybrid feedback optimization model \mathcal{H}_{FO} from (18). From every point in $C \cup D$ there exists a nontrivial solution, and all maximal solutions are complete and not Zeno.

Proof. Since \mathcal{H}_{FO} satisfies Definition 1, we can apply Lemma 5 in Appendix B to establish the claim. Consider an arbitrary $\nu \in C \cup D$, and let U be a neighborhood of ν . We wish to show that $F(\zeta) \cap T_C(\zeta) \neq \emptyset$ for $\zeta \in U \cap C$, where $T_C(\zeta)$ is the tangent cone of the set C at the point ζ . Using the flow map F from (11), we see that only \dot{x} , $\dot{\tau}_g$, and $\dot{\tau}_c$ are non-zero. In addition, C does not restrict x , which implies that x can flow in any direction at any time and remain feasible. Conversely, the timers τ_c and τ_g take values in compact intervals, which implies that some directions are infeasible at some points in time. Therefore, the satisfaction of the condition $F(\zeta) \cap T_C(\zeta) \neq \emptyset$ is determined by the dynamics of τ_c and τ_g .

To show that $F(\zeta) \cap T_C(\zeta) \neq \emptyset$, we compute the tangent cone as

$$T_C(\zeta) := \begin{cases} \mathbb{R}^{n+2m+p} \times \{-1\} \times \mathbb{R} \times \{0\} & \text{if } \tau_c = \tau_{c,max} \\ & \text{and } \tau_g \in (0, \tau_{g,comp}) \\ \mathbb{R}^{n+2m+p} \times \{-1\} \times \{1\} \times \{0\} & \text{if } \tau_c = \tau_{c,max} \\ & \text{and } \tau_g = 0 \\ \mathbb{R}^{n+2m+p} \times \{1\} \times \{-1\} \times \{0\} & \text{if } \tau_c = 0 \\ & \text{and } \tau_g = \tau_{g,comp} \\ \mathbb{R}^{n+2m+p} \times \mathbb{R} \times \{-1\} \times \{0\} & \text{if } \tau_g = \tau_{g,comp} \\ & \text{and } \tau_c \in (\tau_{c,min}, \tau_{c,max}) \\ \mathbb{R}^{n+2m+p} \times \{-1\} \times \{-1\} \times \{0\} & \text{if } \tau_c = \tau_{c,max} \\ & \text{and } \tau_g = \tau_{g,comp} \\ \mathbb{R}^{n+2m+p} \times \{1\} \times \{1\} \times \{0\} & \text{if } \tau_c = 0 \\ & \text{and } \tau_g = 0 \\ \mathbb{R}^{n+2m+p} \times \mathbb{R} \times \mathbb{R} \times \{0\} & \text{else.} \end{cases}$$

By inspection, it holds that $F(\zeta) \in T_C(\zeta)$ for each $\zeta \in C$, which implies that condition (VC) from Lemma 5 is satisfied for every $\nu \in C \cup D$. Then there exists a nontrivial solution ϕ to \mathcal{H}_{FO} with $\phi(0,0) = \nu$. Let $\mathcal{S}_{\mathcal{H}_{FO}}$ denote the set of all such solutions. Since (VC) from Lemma 5 holds for every $\nu \in C \cup D$, it also holds for every $\nu \in C \setminus D$, and

therefore there exists a nontrivial solution from every initial point in $C \cup D$, and every $\phi \in \mathcal{H}_{FO}$ satisfies one of the three conditions of Lemma 5.

By inspection, we have $G(D) \subset C \cup D$, which implies that 3) in Lemma 5 does not occur. Regarding 2), during flows, the components of the solution that change are x, τ_c, τ_g , and thus only their boundedness needs to be verified. Since τ_c and τ_g are in compact sets, they are bounded and cannot blow up to infinity. And since $u \in \mathcal{U}$, which is a compact set, we see that u is bounded, and there exists some finite $u_{max} \geq 0$ such that $\|u\| \leq u_{max}$. Since the mapping $(x, u) \mapsto Ax + Bu$ is Lipschitz, F in (11) is globally Lipschitz. This property and the boundedness of inputs together imply that Condition 2) from Lemma 5 does not hold. Therefore, Condition 1) from Lemma 5 does hold, and all maximal solutions to \mathcal{H}_{FO} are complete.

Since resets by G are triggered only when either one of the timers have reached zero, and it resets any timers that have reached zero to constant non-zero values, $G(D) \cap D = \emptyset$, which rules out Zeno behavior by Proposition 2.34 in [19]. Then all maximal solutions are complete and non-Zeno. \square

B. Algorithm Framework

To initialize the system, $x(0,0)$ is given, $u(0,0)$ is user-specified, $y_s(0,0) = Hu(0,0) + d$ is measured, and we impose the following restrictions: (i) $z(0,0)$ is set equal to $u(0,0)$, (ii) $\tau_c(0,0) \in [\tau_{c,min}, \tau_{c,max}]$ where $0 < \tau_{c,min} < \tau_{c,max}$ are user-specified bounds, (iii) $\tau_g(0,0) = \tau_{g,comp}$, where $\tau_{g,comp} > 0$ is user-specified, and (iv) $\ell(0,0) = 0$.

While the hybrid system \mathcal{H}_{FO} runs, its state will remain in the flow set unless one of the conditions for a jump is satisfied, in which case \mathcal{H}_{FO} will jump via one of three cases in (14). Case (i) in (14) performs a gradient descent update but does not change the input to the system and does not sample the output, Case (ii) in (14) applies the most recent iterate of the optimization algorithm as the input to the LTI system and measures the LTI system's output, and Case (iii) in (14) combines Cases (i) and (ii).

To examine the evolution of a solution over time, consider an initial condition ν that satisfies

$$\begin{aligned} y_s(0,0) &= Hu(0,0) + d, z(0,0) = u(0,0), \\ \tau_c(0,0) &\in [\tau_{c,min}, \tau_{c,max}], \tau_g(0,0) = \tau_{g,comp}, \ell(0,0) = 0, \end{aligned} \quad (19)$$

and consider a solution ϕ to \mathcal{H}_{FO} with initial condition $\phi(0,0) = \nu$. After the initial input to the system $u(0,0)$ is applied, the system performs $\alpha(0)$ gradient descent iterations (which are $\alpha(0)$ Case (i) jumps) before the input to the LTI system is changed, and we use $\alpha(i)$ to denote the number of gradient descent iterations that are performed when computing the $(i+1)^{th}$ value of the input u . Section III-D required that $2\tau_{g,comp} \leq \tau_{c,min}$ and therefore at least two gradient descent iterations are performed between consecutive changes in the value of u , which implies that $\alpha(i) \geq 2$ for all $i \geq 0$.

The initial condition for these iterates is $z_0(0,0) = u(0,0)$, and the k^{th} such iterate is denoted $z_k(t_k, k)$. After $u(0,0)$ is

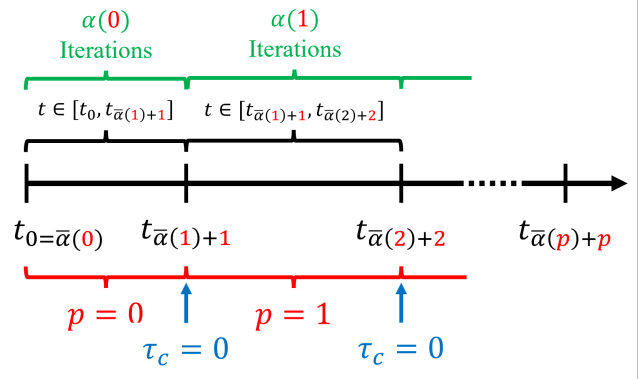


Fig. 2. A visual representation of the continuous time flow of \mathcal{H}_{FO} in terms of p .

applied as the input to the LTI system and before u jumps for the first time, the iterate $z_{\alpha(0)}(t_{\alpha(0)}, \alpha(0))$ is computed, and the hybrid time $(t_{\alpha(0)}, \alpha(0))$ reflects the fact that $\alpha(0)$ Case (i) jumps have occurred. Then, when the value of u changes for the first time (which corresponds to a Case (ii) jump), its next value is set equal to the optimization iterate that was just computed, i.e.,

$$u(t_{\alpha(0)+1}, \alpha(0) + 1) = z_{\alpha(0)}(t_{\alpha(0)}, \alpha(0)).$$

This same Case (ii) jump sets the initial iterate for the computation of the next input as

$$z_0(t_{\alpha(0)+1}, \alpha(0) + 1) = z_{\alpha(0)}(t_{\alpha(0)}, \alpha(0)),$$

i.e., the initial iterate when computing the next input is set equal to the final iterate that was generated when computing the previous input. This pattern is illustrated in Figure 2.

We can identify the general pattern that occurs at an arbitrary Case (i) jump. Suppose that p total Case (ii) jumps have occurred so far. Then, when a Case (i) jump occurs, an optimization iteration of the form

$$\begin{aligned} z_{k+1}(t_{\bar{\alpha}(p)+p+k+1}, \bar{\alpha}(p) + p + k + 1) = \\ \Pi_{\mathcal{U}}[z_k(t_{\bar{\alpha}(p)+p+k}, \bar{\alpha}(p) + p + k) \\ - \nabla_u \Phi(z_k(t_{\bar{\alpha}(p)+p+k}, \bar{\alpha}(p) + p + k))] \end{aligned} \quad (20)$$

is computed, where $k+1 \leq \alpha(p+1)$, and where for ease of notation we have suppressed the y_s term. We use $\bar{\alpha}(p)$ to denote the total number of gradient descent iterations that have been computed for any input up until the p^{th} jump in u . That is,

$$\bar{\alpha}(p) = \begin{cases} \bar{\alpha}(p-1) + \alpha(p-1) & p \geq 1 \\ 0 & \text{otherwise,} \end{cases}$$

where $\bar{\alpha}(p-1) + \alpha(p-1) = \sum_{i=0}^{p-1} \alpha(i)$ for $p \geq 1$.

We note that the hybrid time index on the left-hand side of (20) has counted $\bar{\alpha}(p) + p + k + 1$ jumps so far, which accounts for $\bar{\alpha}(p)$ total optimization iterations that were computed for all inputs prior to the p^{th} change in the input, p changes in the input, and $k+1$ optimization iterations that have been computed for the next input.

For a Case (ii) jump, the $(p+1)^{th}$ input to the system is set as

$$u(t_{\bar{\alpha}(p)+p}, \bar{\alpha}(p) + p) = z_{\alpha(p-1)}(t_{\bar{\alpha}(p)+p-1}, \bar{\alpha}(p) + p - 1),$$

and the initial iterate for computing the next input is set as

$$z_0(t_{\bar{\alpha}(p)+p}, \bar{\alpha}(p) + p) = z_{\alpha(p-1)}(t_{\bar{\alpha}(p)+p-1}, \bar{\alpha}(p) + p - 1).$$

We observe that Case (i) is triggered by the timer τ_g reaching 0, i.e., $\zeta \in D_1$ from (16), and Case (ii) is triggered by the timer τ_c reaching 0, i.e., $\zeta \in D_2$ from (17). Below, we will examine the evolution of the state x in the system \mathcal{H}_{FO} . When doing so, we will consider truncated hybrid time domains that include a finite number of Case (ii) jumps, which we will use to provide finite-time analyses for the behavior of the state x .

Formally, consider a solution ϕ of \mathcal{H}_{FO} , and define $\theta : \mathcal{U} \times \mathbb{N} \rightarrow \mathbb{N}$ so that $\theta(u, j)$ is equal to the number of jumps in u up to jump j in the domain of ϕ . Then for $P \in \mathbb{N}$ we will consider hybrid time domains of the form

$$\Gamma(\phi, P) := \{(t, j) \in \text{dom } \phi : \theta(u, j) \leq P\}. \quad (21)$$

The final hybrid time in such a hybrid time domain is

$$(t_{\bar{\alpha}(P+1)+P+1}, \bar{\alpha}(P+1) + P)$$

because $\bar{\alpha}(P+1) + P$ total jumps have occurred by the time that u has jumped P times. Of this total, $\bar{\alpha}(P+1)$ jumps are gradient descent iterations and P are jumps in the value of u . The value of continuous time reaches $t_{\bar{\alpha}(P+1)+P+1}$ because the $(\bar{\alpha}(P+1) + P + 1)^{th}$ jump is about to occur at the end of $\Gamma(\phi, P)$.

V. CONVERGENCE ANALYSIS

This section solves Problem 2. We first derive a convergence rate for the iterates of the optimization algorithm in the loop, and then we bound the distance from the states of the system to the origin.

A. State Bounds with Piecewise Constant Inputs

The next result bounds the distance from the state x to the origin as a function of time.

Lemma 2 (Jump-Considered Exponential Convergence). Consider the hybrid system \mathcal{H}_{FO} from (18) and suppose that Assumption 1 holds for it. Let ϕ be a maximal solution to \mathcal{H}_{FO} with initial condition $\phi(0, 0) = \nu$ that satisfies (19), fix $P \in \mathbb{N}$, and consider the associated hybrid time domain $\Gamma(\phi, P)$ defined in (21). Then

$$\begin{aligned} & \|x(t_{\bar{\alpha}(P+1)+P+1}, \bar{\alpha}(P+1) + P)\| \\ & \leq \|e^{A(t_{\bar{\alpha}(P+1)+P+1})} x(0, 0)\| \\ & + \sum_{p=0}^P \int_{t_{\bar{\alpha}(p)+p}}^{t_{\bar{\alpha}(p+1)+p+1}} \|e^{A(t_{\bar{\alpha}(p+1)+p+1}-\tau)} Bu(t_{\bar{\alpha}(p)+p}, \bar{\alpha}(p) + p)\| d\tau, \end{aligned}$$

where we define $t_0 := 0$.

Proof. The model of \mathcal{H}_{FO} applies piecewise constant inputs to the underlying LTI system. Then integrating the underlying LTI dynamics over $\Gamma(\phi, P)$ gives

$$\begin{aligned} & x(t_{\bar{\alpha}(P+1)+P+1}, \bar{\alpha}(P+1) + P) \\ & = e^{A(t_{\bar{\alpha}(P+1)+P+1})} x(0, 0) \\ & + \int_0^{t_{\bar{\alpha}(P+1)+P+1}} e^{t_{\bar{\alpha}(P+1)+P+1}-\tau} Bu(\tau) d\tau \\ & = e^{A(t_{\bar{\alpha}(P+1)+P+1})} x(0, 0) \\ & + \sum_{p=0}^P \int_{t_{\bar{\alpha}(p)+p}}^{t_{\bar{\alpha}(p+1)+p+1}} e^{A(t_{\bar{\alpha}(p+1)+p+1}-\tau)} Bu(t_{\bar{\alpha}(p)+p}, \bar{\alpha}(p) + p) d\tau, \end{aligned}$$

where for each $p \in \{0, \dots, P\}$ the input $u(t_{\bar{\alpha}(p)+p}, \bar{\alpha}(p) + p)$ is constant over the interval $[t_{\bar{\alpha}(p)+p}, t_{\bar{\alpha}(p+1)+p+1}]$. The result then follows from taking the norm of both sides and applying the triangle inequality. \square

B. Input Convergence

We next seek to quantify relationships between successive inputs to the system. Toward doing so, we have the following lemma that relates successive iterates that are used to compute those inputs.

Lemma 3 (Input Convergence Rate). Consider the hybrid system \mathcal{H}_{FO} from (18) and let Assumptions 1 and 2 hold. Let ϕ denote a maximal solution to \mathcal{H}_{FO} with initial condition $\phi(0, 0) = \nu$ that satisfies (19), and for any $P \in \mathbb{N}$ consider the associated hybrid time domain $\Gamma(\phi, P)$ from (21). Then, for any integer $p \in \{0, \dots, P\}$ the state z obeys

$$\begin{aligned} & \|z_{\alpha(p)}(t_{\bar{\alpha}(p)+\alpha(p)+p}, \bar{\alpha}(p) + \alpha(p) + p) \\ & - z^*(t_{\bar{\alpha}(p)+p}, \bar{\alpha}(p) + p)\| \\ & \leq q^{\frac{\alpha(p)-1}{2}} \|z_1(t_{\bar{\alpha}(p)+p}, \bar{\alpha}(p) + p) \\ & - z^*(t_{\bar{\alpha}(p)+p}, \bar{\alpha}(p) + p)\|, \end{aligned}$$

where

$$z^*(t_{\bar{\alpha}(p)+p}, \bar{\alpha}(p) + p) = \arg \min_{u \in \mathcal{U}} \Phi(u, y_s(t_{\bar{\alpha}(p)+p}, \bar{\alpha}(p) + p)),$$

the stepsize is $\gamma \in (0, \frac{2}{\lambda_{\min}(Q_u) + L})$, and

$$q := 1 - 2\gamma\lambda_{\min}(Q_u) + \gamma^2 L^2 \in (0, 1),$$

where L is from (7).

Proof. The steps of the proof follow that of traditional convex optimization literature for the minimization of a strongly convex function. For the hybrid system \mathcal{H}_{FO} , we can quantify convergence of the computation of inputs by examining the distance of an intermediate iterate z from its optimal value after $k+1$ iterations of gradient descent. That

is, we can bound the term

$$\left\| z_{k+1}(t_{\bar{\alpha}(p)+k+1+p}, \bar{\alpha}(p) + k + 1 + p) - z^*(t_{\bar{\alpha}(p)+p}, \bar{\alpha}(p) + p) \right\|^2,$$

where $k+1$ is some number of iterations between 1 and $\alpha(p)$. We can then express z_{k+1} in terms of z_k and use the fact that

$$z^*(t_{\bar{\alpha}(p)+p}, \bar{\alpha}(p) + p) = \Pi_{\mathcal{U}} \left[z^*(t_{\bar{\alpha}(p)+p}, \bar{\alpha}(p) + p) - \gamma \nabla_u \Phi(z^*(t_{\bar{\alpha}(p)+p}, \bar{\alpha}(p) + p), y_s(t_{\bar{\alpha}(p)+p}, \bar{\alpha}(p) + p)) \right],$$

i.e., $z^*(t_{\bar{\alpha}(p)+p}, \bar{\alpha}(p) + p)$ is a fixed point of the projected gradient descent update law. Doing so gives

$$\begin{aligned} & \left\| z_{k+1}(t_{\bar{\alpha}(p)+k+1+p}, \bar{\alpha}(p) + k + 1 + p) - z^*(t_{\bar{\alpha}(p)+p}, \bar{\alpha}(p) + p) \right\|^2 \\ &= \left\| \Pi_{\mathcal{U}} \left[z_k(t_{\bar{\alpha}(p)+k+p}, \bar{\alpha}(p) + k + p) - \gamma \nabla_u \Phi(z_k(t_{\bar{\alpha}(p)+k+p}, \bar{\alpha}(p) + k + p)) \right] - \Pi_{\mathcal{U}} \left[z^*(t_{\bar{\alpha}(p)+p}, \bar{\alpha}(p) + p) - \gamma \nabla_u \Phi(z^*(t_{\bar{\alpha}(p)+p}, \bar{\alpha}(p) + p)) \right] \right\|^2, \end{aligned}$$

where for ease of notation we have used

$$\nabla_u \Phi(z_k(t_{\bar{\alpha}(p)+k+p}, \bar{\alpha}(p) + k + p)) := \nabla_u \Phi(z_k(t_{\bar{\alpha}(p)+k+p}, \bar{\alpha}(p) + k + p), y_s(t_{\bar{\alpha}(p)+p}, \bar{\alpha}(p) + p)),$$

and similar for $\nabla_u \Phi(z^*(t_{\bar{\alpha}(p)+p}, \bar{\alpha}(p) + p))$. The non-expansive property of $\Pi_{\mathcal{U}}$ lets us remove the projections and attain an upper bound. Doing this and expanding gives

$$\begin{aligned} & \left\| z_{k+1}(t_{\bar{\alpha}(p)+k+1+p}, \bar{\alpha}(p) + k + 1 + p) - z^*(t_{\bar{\alpha}(p)+p}, \bar{\alpha}(p) + p) \right\|^2 \\ & \leq \left\| z_k(t_{\bar{\alpha}(p)+k+p}, \bar{\alpha}(p) + k + p) - z^*(t_{\bar{\alpha}(p)+p}, \bar{\alpha}(p) + p) \right\|^2 \\ & \quad - 2\gamma \left(z_k(t_{\bar{\alpha}(p)+k+p}, \bar{\alpha}(p) + k + p) - z^*(t_{\bar{\alpha}(p)+p}, \bar{\alpha}(p) + p) \right)^\top \cdot \\ & \quad \left(\nabla_u \Phi(z_k(t_{\bar{\alpha}(p)+k+p}, \bar{\alpha}(p) + k + p)) - \nabla_u \Phi(z^*(t_{\bar{\alpha}(p)+p}, \bar{\alpha}(p) + p)) \right) \\ & \quad + \gamma^2 \left\| \nabla_u \Phi(z_k(t_{\bar{\alpha}(p)+k+p}, \bar{\alpha}(p) + k + p)) - \nabla_u \Phi(z^*(t_{\bar{\alpha}(p)+p}, \bar{\alpha}(p) + p)) \right\|^2. \end{aligned}$$

Using the L -Lipschitz property of $\nabla \Phi_u$ from (7), we find

$$\begin{aligned} & \left\| z_{k+1}(t_{\bar{\alpha}(p)+k+1+p}, \bar{\alpha}(p) + k + 1 + p) - z^*(t_{\bar{\alpha}(p)+p}, \bar{\alpha}(p) + p) \right\|^2 \\ & \leq \left\| z_k(t_{\bar{\alpha}(p)+k+p}, \bar{\alpha}(p) + k + p) - z^*(t_{\bar{\alpha}(p)+p}, \bar{\alpha}(p) + p) \right\|^2 \\ & \quad - 2\gamma \left(z_k(t_{\bar{\alpha}(p)+k+p}, \bar{\alpha}(p) + k + p) - z^*(t_{\bar{\alpha}(p)+p}, \bar{\alpha}(p) + p) \right)^\top \cdot \\ & \quad \left(\nabla_u \Phi(z_k(t_{\bar{\alpha}(p)+k+p}, \bar{\alpha}(p) + k + p)) - \nabla_u \Phi(z^*(t_{\bar{\alpha}(p)+p}, \bar{\alpha}(p) + p)) \right) \\ & \quad + \gamma^2 L^2 \left\| z_k(t_{\bar{\alpha}(p)+k+p}, \bar{\alpha}(p) + k + p) - z^*(t_{\bar{\alpha}(p)+p}, \bar{\alpha}(p) + p) \right\|^2. \end{aligned}$$

Then, by using the $\lambda_{\min}(Q_u)$ -strong convexity property of Φ from (6), we find

$$\begin{aligned} & \left\| z_{k+1}(t_{\bar{\alpha}(p)+k+1+p}, \bar{\alpha}(p) + k + 1 + p) - z^*(t_{\bar{\alpha}(p)+p}, \bar{\alpha}(p) + p) \right\|^2 \\ & \leq \left\| z_k(t_{\bar{\alpha}(p)+k+p}, \bar{\alpha}(p) + k + p) - z^*(t_{\bar{\alpha}(p)+p}, \bar{\alpha}(p) + p) \right\|^2 \\ & \quad - 2\gamma \lambda_{\min}(Q_u) \left\| z_k(t_{\bar{\alpha}(p)+k+p}, \bar{\alpha}(p) + k + p) - z^*(t_{\bar{\alpha}(p)+p}, \bar{\alpha}(p) + p) \right\|^2 \\ & \quad + \gamma^2 L^2 \left\| z_k(t_{\bar{\alpha}(p)+k+p}, \bar{\alpha}(p) + k + p) - z^*(t_{\bar{\alpha}(p)+p}, \bar{\alpha}(p) + p) \right\|^2, \end{aligned}$$

which simplifies to

$$\begin{aligned} & \left\| z_{k+1}(t_{\bar{\alpha}(p)+k+1+p}, \bar{\alpha}(p) + k + 1 + p) - z^*(t_{\bar{\alpha}(p)+p}, \bar{\alpha}(p) + p) \right\|^2 \\ & \leq (1 - 2\gamma \lambda_{\min}(Q_u) + \gamma^2 L^2) \left\| z_k(t_{\bar{\alpha}(p)+k+p}, \bar{\alpha}(p) + k + p) - z^*(t_{\bar{\alpha}(p)+p}, \bar{\alpha}(p) + p) \right\|^2 \\ & = q \left\| z_k(t_{\bar{\alpha}(p)+k+p}, \bar{\alpha}(p) + k + p) - z^*(t_{\bar{\alpha}(p)+p}, \bar{\alpha}(p) + p) \right\|^2. \quad (22) \end{aligned}$$

To ensure that $q \in (0, 1)$, we use [20, Theorem 2.1.15], which shows that $\gamma \in \left(0, \frac{2}{\lambda_{\min}(Q_u) + L}\right)$ gives $q \in (0, 1)$. Then iteratively applying (22) and taking the square root completes the proof. \square

C. Complete Hybrid Convergence

The next result is our main result and it gives an upper bound on the distance from the state of the underlying LTI system, namely x , to the origin as a function of each input that is applied to the system and the unknown disturbance d . For this result, we upper-bound the distance from the state of the system \mathcal{H}_{FO} to the set

$$\mathcal{A} = B_r(0) \times \mathcal{U} \times \mathbb{R}^p \times \mathbb{R}^m \times \mathbb{R} \times \mathbb{R} \times \mathbb{N},$$

where

$$r = \frac{M \|B\| u_{max}}{\rho} + \frac{M \|B\| q^{\frac{1}{2}}}{\rho} \left(d_{\mathcal{U}} + \gamma \left(\|H^{\top} d\| + \|I_m + H^{\top} H\| u_{max} \right) \right),$$

where $M > 0$ is a constant,

$$\rho = \min_{i \in \{1, \dots, n\}} |\Re\{\lambda_i(A)\}|, \quad (23)$$

and where A is from the hybrid model \mathcal{H}_{FO} in (18).

Theorem 1 (Complete Hybrid Convergence). Consider the hybrid system \mathcal{H}_{FO} from (18) and suppose that Assumptions 1 and 2 hold. Let ϕ denote a maximal solution to \mathcal{H}_{FO} with initial condition $\phi(0, 0) = \nu$ that satisfies (19), and for a fixed $P \in \mathbb{N}$ consider the associated hybrid time domain $\Gamma(\phi, P)$ from (21). Then

$$\begin{aligned} & \|\phi(t_{\bar{\alpha}(P+1)+P+1}, \bar{\alpha}(P+1) + P)\|_{\mathcal{A}} \\ & \leq M \exp(-\rho(t_{\bar{\alpha}(P+1)+P+1})) \|x(0, 0)\| \\ & + \frac{M \|B\| u_{max}}{\rho} \exp(-\rho(t_{\bar{\alpha}(P+1)+P+1})) \\ & + \frac{M \|B\| q^{\frac{1}{2}}}{\rho} \exp(-\rho(t_{\bar{\alpha}(P+1)+P+1})) \cdot \\ & \left(d_{\mathcal{U}} + \gamma \left(\|H^{\top} d\| + \|Q_u + H^{\top} Q_y H\| u_{max} \right) \right), \end{aligned}$$

where $u_{max} := \max_{u \in \mathcal{U}} \|u\|$ is the maximum norm of a feasible input, $d_{\mathcal{U}} = \max_{u_1, u_2 \in \mathcal{U}} \|u_1 - u_2\|$ is the diameter of the set \mathcal{U} , ρ is from (23), and $M > 0$ is a constant.

Proof. By definition of \mathcal{A} , only the state x in ϕ affects the value of $\|\phi(t, j)\|_{\mathcal{A}}$. That is, we have

$$\begin{aligned} & \|\phi(t_{\bar{\alpha}(P+1)+P+1}, \bar{\alpha}(P+1) + P)\|_{\mathcal{A}} \\ & = \|x(t_{\bar{\alpha}(P+1)+P+1}, \bar{\alpha}(P+1) + P)\|_{B_r(0)}, \quad (24) \end{aligned}$$

and we therefore focus our analysis on x .

Using the system description in Section IV-B, we observe that

$$\begin{aligned} & u(t_{\bar{\alpha}(p)+p}, \bar{\alpha}(p) + p) \\ & = z_{\alpha(p-1)} \left(t_{\bar{\alpha}(p-1)+\alpha(p-1)+p-1}, \right. \\ & \quad \left. \bar{\alpha}(p-1) + \alpha(p-1) + p-1 \right), \end{aligned}$$

where the iterates that are computed to give that input are working towards the optimizer

$$u^*(t_{\bar{\alpha}(p)+p}, \bar{\alpha}(p) + p) = z^* \left(t_{\bar{\alpha}(p-1)+p-1}, \bar{\alpha}(p-1) + p-1 \right),$$

which is defined as

$$\begin{aligned} & u^*(t_{\bar{\alpha}(p)+p}, \bar{\alpha}(p) + p) \\ & = \arg \min_{u \in \mathcal{U}} \Phi \left(u, y_s(t_{\bar{\alpha}(p-1)+p-1}, \bar{\alpha}(p-1) + p-1) \right). \end{aligned}$$

Then, using Lemma 3, we find that

$$\begin{aligned} & \|u(t_{\bar{\alpha}(p)+p}, \bar{\alpha}(p) + p) - u^*(t_{\bar{\alpha}(p)+p}, \bar{\alpha}(p) + p)\| \\ & \leq q^{\frac{\alpha(p-1)-1}{2}} \left\| z_1 \left(t_{\bar{\alpha}(p-1)+p}, \bar{\alpha}(p-1) + p \right) \right. \\ & \quad \left. - z^* \left(t_{\bar{\alpha}(p-1)+p-1}, \bar{\alpha}(p-1) + p-1 \right) \right\| \\ & = q^{\frac{\alpha(p-1)-1}{2}} \left\| z_0 \left(t_{\bar{\alpha}(p-1)+p-1}, \bar{\alpha}(p-1) + p-1 \right) \right. \\ & \quad \left. - \gamma(Q_u + H^{\top} Q_y H) z_0 \left(t_{\bar{\alpha}(p-1)+p-1}, \bar{\alpha}(p-1) + p-1 \right) \right. \\ & \quad \left. - \gamma H^{\top} d - z^* \left(t_{\bar{\alpha}(p-1)+p-1}, \bar{\alpha}(p-1) + p-1 \right) \right\|, \end{aligned}$$

where we have (i) expanded the gradient descent law

$$\begin{aligned} & z_1 \left(t_{\bar{\alpha}(p-1)+p}, \bar{\alpha}(p-1) + p \right) \\ & = \Pi_{\mathcal{U}} \left[z_0 \left(t_{\bar{\alpha}(p-1)+p-1}, \bar{\alpha}(p-1) + p-1 \right) \right. \\ & \quad \left. - \gamma \nabla_u \Phi \left(z_0 \left(t_{\bar{\alpha}(p-1)+p-1}, \bar{\alpha}(p-1) + p-1 \right), \right. \right. \\ & \quad \left. \left. y_s \left(t_{\bar{\alpha}(p-1)+p-1}, \bar{\alpha}(p-1) + p-1 \right) \right) \right], \end{aligned}$$

(ii) substituted

$$\begin{aligned} & z^* \left(t_{\bar{\alpha}(p-1)+p-1}, \bar{\alpha}(p-1) + p-1 \right) \\ & = \Pi_{\mathcal{U}} \left[z^* \left(t_{\bar{\alpha}(p-1)+p-1}, \bar{\alpha}(p-1) + p-1 \right) \right] \end{aligned}$$

and applied the non-expansive property of $\Pi_{\mathcal{U}}$, (iii) used the fact that, under Assumption 2, we have

$$\nabla_u \Phi(u, y_s) = Q_u u + H^{\top} Q_y y_s,$$

and (iv) as described in Remark 1, expanded the sampled output as

$$\begin{aligned} & y_s \left(t_{\bar{\alpha}(p-1)+p-1}, \bar{\alpha}(p-1) + p-1 \right) \\ & = H u(t_{\bar{\alpha}(p-1)+p-1}, \bar{\alpha}(p-1) + p-1) + d \\ & = H z_0(t_{\bar{\alpha}(p-1)+p-1}, \bar{\alpha}(p-1) + p-1) + d. \end{aligned}$$

Next, applying the triangle inequality gives

$$\begin{aligned} & \|u(t_{\bar{\alpha}(p)+p}, \bar{\alpha}(p) + p) - u^*(t_{\bar{\alpha}(p)+p}, \bar{\alpha}(p) + p)\| \\ & \leq q^{\frac{\alpha(p-1)-1}{2}} \left\| z_0 \left(t_{\bar{\alpha}(p-1)+p-1}, \bar{\alpha}(p-1) + p-1 \right) \right. \\ & \quad \left. - z^* \left(t_{\bar{\alpha}(p-1)+p-1}, \bar{\alpha}(p-1) + p-1 \right) \right\| \\ & \quad + \gamma q^{\frac{\alpha(p-1)-1}{2}} \left(\|H^{\top} d\| \right. \\ & \quad \left. + \|(Q_u + H^{\top} Q_y H) z_0 \left(t_{\bar{\alpha}(p-1)+p-1}, \bar{\alpha}(p-1) + p-1 \right)\| \right). \end{aligned}$$

Next, since $z_0(t_{\bar{\alpha}(p-1)+p-1}, \bar{\alpha}(p-1) + p-1) \in \mathcal{U}$, we see that

$$\|z_0(t_{\bar{\alpha}(p-1)+p-1}, \bar{\alpha}(p-1) + p-1)\| \leq u_{max}.$$

Then, applying the triangle inequality again gives

$$\begin{aligned} & \|(Q_u + H^\top Q_y H)z_0(t_{\bar{\alpha}(p-1)+p-1}, \bar{\alpha}(p-1) + p - 1)\| \\ & \leq \|Q_u + H^\top Q_y H\|u_{max}, \end{aligned}$$

which leads to the overall bound

$$\begin{aligned} & \|u(t_{\bar{\alpha}(p)+p}, \bar{\alpha}(p) + p) - u^*(t_{\bar{\alpha}(p)+p}, \bar{\alpha}(p) + p)\| \\ & \leq q^{\frac{\alpha(p-1)-1}{2}} \left(d_{\mathcal{U}} + \gamma \left(\|H^\top d\| + \|Q_u + H^\top Q_y H\|u_{max} \right) \right), \end{aligned} \quad (25)$$

where we have used

$$\begin{aligned} & \|z_0(t_{\bar{\alpha}(p-1)+p-1}, \bar{\alpha}(p-1) + p - 1) \\ & - z^*(t_{\bar{\alpha}(p-1)+p-1}, \bar{\alpha}(p-1) + p - 1)\| \leq d_{\mathcal{U}}. \end{aligned}$$

Now, using the triangle inequality with Lemma 2, we find

$$\begin{aligned} & \|\phi(t_{\bar{\alpha}(P+1)+P+1}, \bar{\alpha}(P+1) + P)\|_{\mathcal{A}} \\ & \leq \|e^{A(t_{\bar{\alpha}(P+1)+P+1})}\| \|x(0, 0)\| \\ & + \sum_{p=0}^P \int_{t_{\bar{\alpha}(p)+p}}^{t_{\bar{\alpha}(p+1)+p+1}} \|e^{A(t_{\bar{\alpha}(p+1)+p+1}-\tau)}\| \\ & \|B\| \left(\|u(t_{\bar{\alpha}(p)+p}, \bar{\alpha}(p) + p) - u^*(t_{\bar{\alpha}(p)+p}, \bar{\alpha}(p) + p)\| \right. \\ & \left. + \|u^*(t_{\bar{\alpha}(p)+p}, \bar{\alpha}(p) + p)\| \right) d\tau. \end{aligned}$$

Then, using (25) and the definition of u_{max} gives

$$\begin{aligned} & \|x(t_{\bar{\alpha}(P+1)+P+1}, \bar{\alpha}(P+1) + P)\| \\ & \leq \|e^{A(t_{\bar{\alpha}(P+1)+P+1})}\| \|x(0, 0)\| \\ & + \sum_{p=0}^P \int_{t_{\bar{\alpha}(p)+p}}^{t_{\bar{\alpha}(p+1)+p+1}} \|e^{A(t_{\bar{\alpha}(p+1)+p+1}-\tau)}\| \|B\| \\ & \left(q^{\frac{\alpha(p-1)-1}{2}} \left(d_{\mathcal{U}} + \gamma \left(\|H^\top d\| + \|Q_u + H^\top Q_y H\|u_{max} \right) \right) \right. \\ & \left. + u_{max} \right) d\tau. \end{aligned} \quad (26)$$

It was noted in Section IV-B that $\alpha(p) \geq 2$ for all p . Using this fact and $q \in (0, 1)$, we have

$$q^{\frac{\alpha(p-1)-1}{2}} \leq q^{\frac{1}{2}}. \quad (27)$$

Then using (27) in (26), we have

$$\begin{aligned} & \|x(t_{\bar{\alpha}(P+1)+P+1}, \bar{\alpha}(P+1) + P)\| \\ & \leq \|e^{A(t_{\bar{\alpha}(P+1)+P+1})}\| \|x(0, 0)\| \\ & + \sum_{p=0}^P \int_{t_{\bar{\alpha}(p)+p}}^{t_{\bar{\alpha}(p+1)+p+1}} \|e^{A(t_{\bar{\alpha}(p+1)+p+1}-\tau)}\| \|B\| \\ & \left[q^{\frac{1}{2}} \left(d_{\mathcal{U}} + \gamma \left(\|H^\top d\| + \|Q_u + H^\top Q_y H\|u_{max} \right) \right) \right. \\ & \left. + u_{max} \right] d\tau, \end{aligned}$$

and rearranging terms gives

$$\begin{aligned} & \|x(t_{\bar{\alpha}(P+1)+P+1}, \bar{\alpha}(P+1) + P)\| \\ & \leq \|e^{A(t_{\bar{\alpha}(P+1)+P+1})}\| \|x(0, 0)\| \\ & + \|B\| \left(q^{\frac{1}{2}} \left(d_{\mathcal{U}} + \gamma \left(\|H^\top d\| + \|Q_u + H^\top Q_y H\|u_{max} \right) \right) \right) \\ & \sum_{p=0}^P \int_{t_{\bar{\alpha}(p)+p}}^{t_{\bar{\alpha}(p+1)+p+1}} \|e^{A(t_{\bar{\alpha}(p+1)+p+1}-\tau)}\| d\tau \\ & + \|B\| u_{max} \sum_{p=0}^P \int_{t_{\bar{\alpha}(p)+p}}^{t_{\bar{\alpha}(p+1)+p+1}} \|e^{A(t_{\bar{\alpha}(p+1)+p+1}-\tau)}\| d\tau. \end{aligned} \quad (28)$$

Next, we observe that

$$\begin{aligned} & \sum_{p=0}^P \int_{t_{\bar{\alpha}(p)+p}}^{t_{\bar{\alpha}(p+1)+p+1}} \|e^{A(t_{\bar{\alpha}(p+1)+p+1}-\tau)}\| d\tau \\ & = \int_0^{t_{\bar{\alpha}(P+1)+P+1}} \|e^{A(t_{\bar{\alpha}(P+1)+P+1}-\tau)}\| d\tau \\ & \leq M \int_0^{t_{\bar{\alpha}(P+1)+P+1}} \exp(-\rho(t_{\bar{\alpha}(P+1)+P+1} - \tau)) d\tau \\ & = \frac{M}{\rho} [1 - \exp(-\rho(t_{\bar{\alpha}(P+1)+P+1}))], \end{aligned} \quad (29)$$

where the inequality follows from Theorem 2 in [21, Chapter 1.9].

Substituting (29) into (28), applying the bound

$$\|e^{A(t_{\bar{\alpha}(P+1)+P+1})}\| \leq M \exp(-\rho(t_{\bar{\alpha}(P+1)+P+1})),$$

and rearranging terms gives

$$\begin{aligned} & \|x(t_{\bar{\alpha}(P+1)+P+1}, \bar{\alpha}(P+1) + P)\| \\ & \leq M \exp(-\rho(t_{\bar{\alpha}(P+1)+P+1})) \|x(0, 0)\| \\ & + \frac{M \|B\| u_{max}}{\rho} [1 - \exp(-\rho(t_{\bar{\alpha}(P+1)+P+1}))] \\ & + \frac{M \|B\| q^{\frac{1}{2}}}{\rho} [1 - \exp(-\rho(t_{\bar{\alpha}(P+1)+P+1}))] \\ & \left(d_{\mathcal{U}} + \gamma \left(\|H^\top d\| + \|Q_u + H^\top Q_y H\|u_{max} \right) \right). \end{aligned}$$

Then the distance from $x(t_{\bar{\alpha}(P+1)+P+1}, \bar{\alpha}(P+1) + P)$ to $B_r(0)$ is bounded by

$$\begin{aligned} & \|x(t_{\bar{\alpha}(P+1)+P+1}, \bar{\alpha}(P+1) + P)\|_{B_r(0)} \\ & \leq M \exp(-\rho(t_{\bar{\alpha}(P+1)+P+1})) \|x(0, 0)\| \\ & + \frac{M \|B\| u_{max}}{\rho} \exp(-\rho(t_{\bar{\alpha}(P+1)+P+1})) \\ & + \frac{M \|B\| q^{\frac{1}{2}}}{\rho} \exp(-\rho(t_{\bar{\alpha}(P+1)+P+1})) \\ & \left(d_{\mathcal{U}} + \gamma \left(\|H^\top d\| + \|Q_u + H^\top Q_y H\|u_{max} \right) \right), \end{aligned}$$

and the result follows by using (24). \square

Theorem 1 bounds the distance from x to the ball $B_r(0)$, and therefore this bound incorporates asymptotic error in x ,

i.e., its steady-state offset from the origin. While Theorem 1 gives a finite-time bound on the state x , we are also interested in its long-run, asymptotic behavior, which we consider next. The following result is essentially a result on practical stability, in the sense that it shows asymptotic convergence of the state x to a ball of finite, known radius r about the origin.

Corollary 1 (Steady-state error bound). Consider the hybrid system \mathcal{H}_{FO} from (18) and suppose that Assumptions 1 and 2 hold. Let ϕ denote a maximal solution to \mathcal{H}_{FO} with $\phi(0, 0) = \nu$, where ν satisfies (19). Then

$$\limsup_{t+j \rightarrow \infty} \|\phi(t, j)\|_{\mathcal{A}} = 0.$$

Proof. We observe that, for the system \mathcal{H}_{FO} , taking the limit as $t+j$ goes to infinity implies that t itself must go to infinity. As well, j must go to infinity, which implies that the number of jumps that occur in u grows arbitrarily large, as does the time of the “last” jump in u , denoted $t_{\bar{\alpha}(P+1)+P+1}$. Then, in particular, we find that

$$\limsup_{t+j \rightarrow \infty} M \exp(-\rho t) \|x(0, 0)\| = 0 \quad (30)$$

and

$$\limsup_{t+j \rightarrow \infty} \exp(-\rho(t_{\bar{\alpha}(P+1)+P+1})) = 0. \quad (31)$$

Using (30) and (31) in Theorem 1 gives the result. \square

If we wish to shrink the value of r , which is an asymptotic error bound, then decreasing the value of $\tau_{c,min}$ (while still satisfying the requirement $2\tau_{g,comp} < \tau_{c,min}$ from Section III-D) achieves this result. Intuitively, a lower $\tau_{c,min}$ implies that the input to the system changes more often. Finally, we observe that shrinking γ likewise shrinks the term $\gamma(\|H^\top d\| + \|I_m + H^\top H\|u_{max})$ but also increases the term $q^{\frac{1}{2}}$, and therefore the choice of stepsize must balance the tradeoff between these two terms.

VI. SIMULATION RESULTS

This section presents simulation results for the hybrid system \mathcal{H}_{FO} from (18).

A. Problem Setup

We consider a two-input, two-output linear system where the dynamics are given by

$$\dot{x} = \begin{bmatrix} -3 & 1 & 1 & 0 \\ 1 & -1 & 0 & 0 \\ 1 & 0 & -2 & 1 \\ 0 & 0 & 1 & -1 \end{bmatrix} \begin{bmatrix} x_1 \\ x_2 \\ x_3 \\ x_4 \end{bmatrix} + \begin{bmatrix} 1 & 0 \\ 0 & 0 \\ 0 & 0 \\ 0 & 0 \end{bmatrix} \begin{bmatrix} u_1 \\ u_2 \end{bmatrix}$$

$$y = \begin{bmatrix} 0 & 0 & 1 & 0 \\ 0 & 0 & 0 & 1 \end{bmatrix} \begin{bmatrix} x_1 \\ x_2 \\ x_3 \\ x_4 \end{bmatrix},$$

where these dynamics are incorporated into the flow map $F(\zeta)$. We also have $x \in \mathbb{R}^4$, the input $u \in \mathbb{R}^2$, and output

$y \in \mathbb{R}^2$. This setup leads to the hybrid system \mathcal{H}_{FO} with states $y_s \in \mathbb{R}^2, u \in \mathbb{R}^2, \tau_c \in \mathbb{R}, \tau_g \in \mathbb{R}$, and $\ell \in \mathbb{N}$.

These dynamics satisfy Assumption 1, which ensures that the linear time-invariant (LTI) system is asymptotically stable, with the real parts of all eigenvalues being negative. The feedback optimization problem that we solve is

$$\begin{aligned} \min_{u, y_s} \quad & \Phi(u, y_s) := \frac{1}{2}\|u\|^2 + \frac{1}{2}\|y_s\|^2 \\ \text{subject to} \quad & y_s = Hu + d \\ & u \in \mathcal{U}, y_s \in \mathbb{R}^2, \end{aligned}$$

where the objective satisfies Assumption 2, and where we use $\mathcal{U} = [-1.25, 1.25]^2$ and $d = (0.2 \ 0.2)^T$.

B. Numerical Results

For simulations, the Hybrid Equations Toolbox (Version 3.0.0.76) was used, along with the initial conditions

$$\begin{aligned} x(0, 0) &= (2, -5, 8, -1)^\top, u(0, 0) = (-1.25, -1.25)^\top, \\ y_s(0, 0) &= (8.2, -0.8)^\top, z(0, 0) = (-1.25, 1.25)^\top, \\ \tau_c(0, 0) &\in (1, 3), \tau_g(0, 0) = \{0.5\}, \ell(0, 0) = \{0\}, \end{aligned} \quad (32)$$

with stepsize $\gamma = 0.15 \leq \frac{2}{L+\beta}$. We see in Figure 3 that all \mathcal{H}_{FO} states converge towards a value near 0, except for y_s , which remains affected by the constant disturbance from the system output. In particular, because of the disturbance d , the values of x and u do not reach 0 exactly, but instead x converges to $(-0.0379, -0.0379, -0.0379, -0.0379)^\top$ and u converges to $(-0.0379, 0)^\top$.

Given that the disturbance in each coordinate is 0.2, we see that the states of the system have asymptotic error that is approximately 19% of the magnitude of the disturbances in the system, which indicates that hybrid feedback optimization is successfully mitigating disturbances.

VII. CONCLUSION

This paper presented a hybrid system framework for feedback optimization that considers continuous-time dynamics with discrete-time optimization. Using this framework, we develop a hybrid model that applies a feedback optimization formulation and showed that every solution to this model is well-posed, and that its maximal solutions are complete and non-Zeno. We also bounded the convergence of the state of the underlying dynamical system, as well as the rate of convergence of inputs that are computed in the feedback loop. From simulations we were able to see that the system converges to an error ball about the origin, which indicates that feedback optimization is successfully mitigating the effects of disturbances in the system. Future work includes incorporating a time-varying objective function into the underlying optimization problem, as well as using hybrid feedback optimization for systems with nonlinear dynamics.

REFERENCES

- [1] A. Hauswirth, Z. He, S. Bolognani, G. Hug, and F. Dörfler, “Optimization algorithms as robust feedback controllers,” 2024.
- [2] M. Colombino, E. Dall’Anese, and A. Bernstein, “Online optimization as a feedback controller: Stability and tracking,” IEEE TRANSACTIONS ON CONTROL OF NETWORK SYSTEMS, 2020.

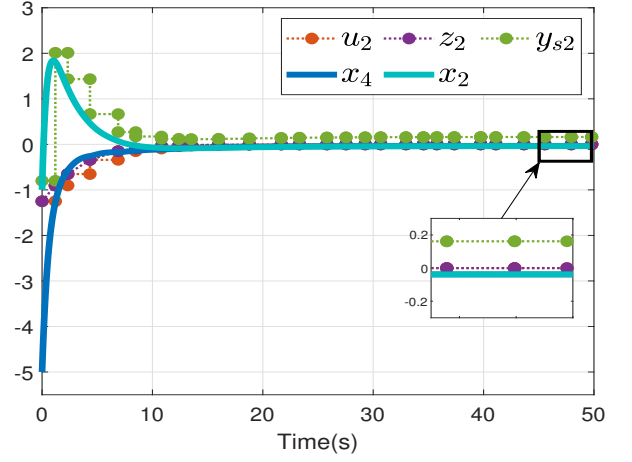
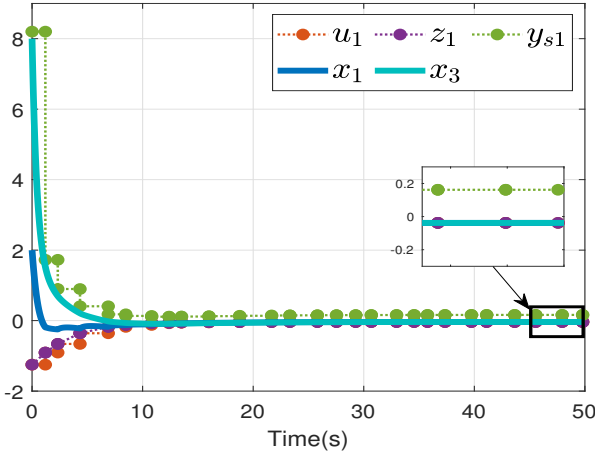


Fig. 3. Convergence of the states of the system \mathcal{H}_{FO} from the initial condition in (32); for clarity, plots of the states have been split into two plots, and the jumps that occur when $\tau_c = 0$ have been omitted. All states converge to values close to zero, which illustrates that the use of feedback optimization largely mitigates the effects of the disturbance d in the hybrid context that we consider.

- [3] W. Wang, Z. He, G. Belgioioso, S. Bolognani, and F. Dörfler, “Decentralized feedback optimization via sensitivity decoupling: Stability and sub-optimality,” 2023.
- [4] L. Ortmann, A. Hauswirth, I. Caduff, F. Dörfler, and S. Bolognani, “Experimental validation of feedback optimization in power distribution grids,” *Electric Power Systems Research*, vol. 189, p. 106782, 2020. [Online]. Available: <https://www.sciencedirect.com/science/article/pii/S037877962030585X>
- [5] G. Behrendt, M. Longmire, Z. I. Bell, and M. Hale, “Distributed asynchronous discrete-time feedback optimization,” *IEEE Transactions on Automatic Control*, pp. 1–16, 2024.
- [6] A. Hauswirth, S. Bolognani, G. Hug, and F. Dörfler, “Timescale separation in autonomous optimization,” *IEEE Transactions on Automatic Control*, vol. 66, no. 2, pp. 611–624, 2021.
- [7] W. Wang, Z. He, G. Belgioioso, S. Bolognani, and F. Dörfler, “Online feedback optimization over networks: A distributed model-free approach,” 2024.
- [8] M. Ellis, H. Durand, and P. D. Christofides, “A tutorial review of economic model predictive control methods,” *Journal of Process Control*, vol. 24, no. 8, pp. 1156–1178, 2014, economic nonlinear model predictive control. [Online]. Available: <https://www.sciencedirect.com/science/article/pii/S0959152414000900>
- [9] D. K. Molzahn, F. Dörfler, H. Sandberg, S. H. Low, S. Chakrabarti, R. Baldick, and J. Lavaei, “A survey of distributed optimization and control algorithms for electric power systems,” *IEEE Transactions on Smart Grid*, vol. 8, no. 6, pp. 2941–2962, 2017.
- [10] D. Krishnamoorthy and S. Skogestad, “Real-time optimization as a feedback control problem – a review,” *Computers & Chemical Engineering*, vol. 161, p. 107723, 2022. [Online]. Available: <https://www.sciencedirect.com/science/article/pii/S0098135422000655>
- [11] S. Menta, A. Hauswirth, S. Bolognani, G. Hug, and F. Dörfler, “Stability of dynamic feedback optimization with applications to power systems,” in *2018 56th Annual Allerton Conference on Communication, Control, and Computing (Allerton)*, 2018, pp. 136–143.
- [12] L. S. P. Lawrence, J. W. Simpson-Porco, and E. Mallada, “Linear-convex optimal steady-state control,” *IEEE Transactions on Automatic Control*, vol. 66, no. 11, pp. 5377–5384, 2021.
- [13] R. A. Horn and C. R. Johnson, *Matrix analysis*. Cambridge University Press, 2012.
- [14] K. R. Hendrickson, D. M. Hustig-Schultz, M. T. Hale, and R. G. Sanfelice, “Exponentially converging distributed gradient descent with intermittent communication via hybrid methods,” in *2021 60th IEEE Conference on Decision and Control (CDC)*, 2021, pp. 1186–1191.
- [15] D. M. Hustig-Schultz, K. Hendrickson, M. Hale, and R. G. Sanfelice, “A totally asynchronous block-based heavy ball algorithm for convex optimization,” in *2023 American Control Conference (ACC)*, 2023, pp. 873–878.
- [16] K. R. Hendrickson, D. M. Hustig-Schultz, M. T. Hale, and R. G. Sanfelice, “Distributed nonconvex optimization with exponential convergence rate via hybrid systems methods,” 2025. [Online]. Available: <https://arxiv.org/abs/2502.02597>
- [17] B. Altun, P. Ojaghi, and R. G. Sanfelice, “A model predictive control framework for hybrid dynamical systems,” *IFAC-PapersOnLine*, vol. 51, no. 20, pp. 128–133, 2018, 6th IFAC Conference on Nonlinear Model Predictive Control NMPC 2018. [Online]. Available: <https://www.sciencedirect.com/science/article/pii/S2405896318326582>
- [18] R. Goebel, R. G. Sanfelice, and A. R. Teel, *Hybrid Dynamical Systems: Modeling, Stability, and Robustness*. New Jersey: Princeton University Press, 2012.
- [19] R. G. Sanfelice, *Hybrid Feedback Control*. New Jersey: Princeton University Press, 2021.
- [20] Y. Nesterov, *Lectures on Convex Optimization*, 2nd ed. Springer Publishing Company, Incorporated, 2018.
- [21] L. Perko, *Differential equations and dynamical systems*. Springer Science & Business Media, 2013, vol. 7.

APPENDIX

A. Outer Semicontinuity of Jump Maps

Lemma 4 ([19, Lemma A.33]). Given closed sets $D_1 \subset \mathbb{R}^m$ and $D_2 \subset \mathbb{R}^m$ and the set-valued maps $G_1 : D_1 \rightrightarrows \mathbb{R}^n$ and $G_2 : D_2 \rightrightarrows \mathbb{R}^n$ that are outer semicontinuous and locally bounded relative to D_1 and D_2 , respectively, the set-valued map $G : D \rightrightarrows \mathbb{R}^n$ given by

$$G(\zeta) := G_1(\zeta) \cup G_2(\zeta) = \begin{cases} G_1(\zeta) & \text{if } \zeta \in D_1 \setminus D_2 \\ G_2(\zeta) & \text{if } \zeta \in D_2 \setminus D_1 \\ G_1(\zeta) \cup G_2(\zeta) & \text{if } \zeta \in D_1 \cap D_2 \end{cases}$$

for each $\zeta \in D$ is outer-semicontinuous and locally bounded relative to the closed set D .

B. Completeness of Maximal Solutions

Lemma 5 (Basic existence of solutions revisited; Proposition 2.34 in [19]). Let $\mathcal{H} = (C, F, D, G)$ satisfy Definition 1. Take an arbitrary $\zeta \in C \cup D$. If $\zeta \in D$ or (VC) there exists a neighborhood U of ζ such that for every $x \in U \cap C$,

$$F(x) \cap T_C(x) \neq \emptyset,$$

then there exists a nontrivial solution ϕ to \mathcal{H} with $\phi(0, 0) = \zeta$. If (VC) holds for every $\zeta \in C \setminus D$, then there exists a nontrivial solution to \mathcal{H} from every initial point in $C \cup D$, and every maximal solution ϕ to \mathcal{H} satisfies exactly one of the following conditions:

- 1) ϕ is complete;
- 2) $\text{dom } \phi$ is bounded and the interval I^J , where $J = \sup_j \text{dom } \phi$, has nonempty interior and $t \mapsto \phi(t, J)$ is a maximal solution to $\dot{z} \in F(z)$, in fact $\lim_{t \rightarrow T} |\phi(t, J)| = \infty$, where $T = \sup_t \text{dom } \phi$;
- 3) $\phi(T, J) \in C \cup D$, where $(T, J) = \sup \text{dom } \phi$.

Furthermore, if $G(D) \subset C \cup D$, then 3) above does not occur.